tvst

Article

Detection of Subclinical Keratoconus With a Validated Alternative Method to Corneal Densitometry

Alejandra Consejo[1,2], Marta Jiménez-García[3,4], Ikram Issarti[3,4], and Jos J. Rozema[3,4]

[1] Department of Applied Physics, University of Zaragoza, Zaragoza, Spain
[2] Institute of Physical Chemistry, Polish Academy of Sciences, Warsaw, Poland
[3] Department of Ophthalmology, Antwerp University Hospital, Edegem, Belgium
[4] Department of Medicine and Health Sciences, University of Antwerp, Antwerp, Belgium

Correspondence: Alejandra Consejo, Department of Applied Physics, University of Zaragoza, C/Pedro Cerbuna 12, 50009 Zaragoza, Spain. e-mail: alejandra.consejo@unizar.es

Received: March 4, 2021
Accepted: July 1, 2021
Published: August 26, 2021

Keywords: keratoconus; subclinical keratoconus; forme fruste; densitometry; statistical image analysis

Citation: Consejo A, Jiménez-García M, Issarti I, Rozema JJ. Detection of subclinical keratoconus with a validated alternative method to corneal densitometry. Transl Vis Sci Technol. 2021;10(9):32, https://doi.org/10.1167/tvst.10.9.32

Purpose: To enhance the current standards of subclinical keratoconus screening based on the statistical modeling of the pixel intensity distribution of Scheimpflug images.

Methods: Scheimpflug corneal tomographies corresponding to 25 corneal meridians of 60 participants were retrospectively collected and divided into three groups: controls (20 eyes), subclinical keratoconus (20 eyes), and clinical keratoconus (20 eyes). Only right eyes were selected. After corneal segmentation, pixel intensities of the stromal tissue were statistically modeled using a Weibull probability density function from which parameter α (pixel brightness) was derived. Further, data were transformed to polar coordinates, smoothed, and interpolated to build a map of the corneal α parameter. The discriminative power of the method was analyzed using receiver operating characteristic curves.

Results: The proposed platform-independent method achieved a higher performance in discriminating subclinical keratoconus from control eyes (90.0% sensitivity, 95.0% specificity, 0.97 area under the curve [AUC]) than the standard method (Belin–Ambrósio enhanced ectasia display), which uses only corneal morphometry (85.0% sensitivity, 85.0% specificity, 0.80 AUC).

Conclusions: Analysis of light backscatter at the cornea successfully discriminates subclinical keratoconus from control eyes, upgrading the results previously reported in the literature.

Translational Relevance: The proposed methodology has the potential to support clinicians in the detection of keratoconus before showing clinical signs.

Introduction

Keratoconus is the most common ectatic corneal disease associated with a progressive thinning of the cornea. The reported prevalence of keratoconus in the general population is 1/1000,[1] although a recent nationwide study reported that it could be as high as 1/375.[2] If untreated, this disease becomes the second leading cause of corneal transplants worldwide.[3] In corneal refractive surgery, detection of the earlier forms of keratoconus is of great importance to prevent iatrogenic postoperative corneal ectasia.[4–6] Although the importance of subclinical keratoconus detection to avoid complications after refractive surgery was already acknowledged two decades ago,[7,8] difficulties remain in its diagnosis due to a lack of definitive methods and criteria for discriminating these early or abortive forms of ectasia from normal corneas.[9]

Scheimpflug-based corneal tomography is considered the gold standard for keratoconus screening. Even though traditional morphological features such as corneal thickness, curvature, or elevation successfully detect clinical keratoconus,[10] their usefulness when detecting subclinical keratoconus is limited.[11]

To overcome the current screening limitations, Koc and colleagues[12] analyzed the asymptomatic eyes of patients with very asymmetric ectasia (n = 38) and concluded that densitometric analysis might detect subclinical keratoconus earlier than

topographic, topometric, and tomographic analyses.[12] Densitometry is an objective and automatic tool to measure corneal transparency. Despite the promising results in discriminating eyes with subclinical keratoconus from normal eyes, the parameter with the highest area under the curve (AUC = 0.883) reported obtained a sensitivity of 75%, which is insufficient for widespread clinical use.[12] Recently, and in agreement with the findings of Lopes et al.,[13] our group reported that densitometry might be used to accurately demarcate the location of clinical keratoconus.[14] One of the major drawbacks of densitometry, however, is that, to date, it is exclusively available on one single commercial device. To overcome this limitation, our research group introduced densitometry distribution analysis (DDA),[15] which is a platform-independent methodology based on the statistical modeling of the pixel intensity distribution of Scheimpflug images that correlates very well with traditional densitometry (overall cornea, $r = 0.89$; $P < 0.001$).[15]

DDA is being developed as a promising tool to help clinicians to diagnose and study various eye conditions, including corneal ectasia,[16,17] corneal hypoxia,[18,] and corneal aging.[15] In particular, DDA has already proven to discriminate early keratoconus without misclassification based on a single Scheimpflug image.[17] In this context, the current work aims to enhance the current standards of subclinical keratoconus screening.

Methodology

Participants

Corneal tomographies were retrospectively collected from two previous studies that took place at the Antwerp University Hospital Ophthalmology department.[19,20] Both studies were approved by the Antwerp University Hospital Research Ethics Committee and adhered to the tenets of the Declaration of Helsinki. All subjects gave written informed consent to participate after the nature and possible consequences of the study were explained.

Sixty right eyes (60 participants) were included in this study (29.2 ± 6.2 years of age). Participants were divided into three groups: controls (20 eyes), clinical keratoconus (20 eyes), and subclinical keratoconus (20 eyes), considered to be the non-pathological eye of a keratoconus patient.[21] The three groups were defined as follows:

1. Control—No slit-lamp findings suggestive of corneal ectasia and normal tomography.
2. Keratoconus—Clinical and tomographic signs consistent with keratoconus (e.g., anterior and/or posterior corneal steepening, corneal thinning, stromal thinning, Fleischer ring at the cone base, Vogt striae). All of the patients were diagnosed by a cornea specialist in a tertiary center.[22]
3. Subclinical keratoconus—Contralateral, asymptomatic eye showing no clinical signs of ectasia of a subject with clinical ectasia in the other eye as a very or highly asymmetric ectasia.[22] These eyes had central average keratometry < 47.2 diopter, KISA% < 100% (18 out of 20 KISA% < 60%),[23] and normal scores for topographical keratoconus classification and ABCD (A0B0C0).[24]

Besides prior crosslinking, other exclusion criteria were corneal scarring, known retinal or corneal pathologies (apart from keratoconus), known ocular procedures or treatments, and known systemic diseases (e.g., diabetes, HIV/AIDS, hypertension). Participants were asked not to use their contact lenses the day they visited the clinic to avoid short-term induced changes by scleral lens wear.[18] To avoid inter-eye correlation, a single eye was chosen from every participant.

The sample size was derived from previously published data on statistical light intensity distribution in Scheimpflug images. The same methodology applied to the current work suggested that a sample size of 10 control and 10 keratoconus participants would yield a 90% power to distinguish between control and keratoconus eyes at the 0.05 significance level.[16]

All participants underwent a comprehensive ophthalmologic examination, including corneal imaging using a Pentacam HR (Oculus Optikgeräte GmbH, Wetzlar, Germany).

Data Analysis

In addition to extracting corneal parameters provided by the device's software, Scheimpflug images corresponding to 25 corneal meridians (a fixed size of 500 × 1080 pixels) were exported without gamma correction or contrast enhancement for further analysis. This corresponded to a total of 1500 images (i.e., 60 participants and 25 images per participant). Each image was processed in two steps: (1) corneal segmentation and (2) statistical modeling of the pixel brightness distribution, as described in detail elsewhere.[17,18]

In the first step, the anterior and posterior boundaries of the cornea are automatically extracted. After segmentation, a moving region of interest (ROI) was automatically selected for statistical modeling as described elsewhere.[18] In short, the vertical (axial) dimension of the ROI was delimited by anterior

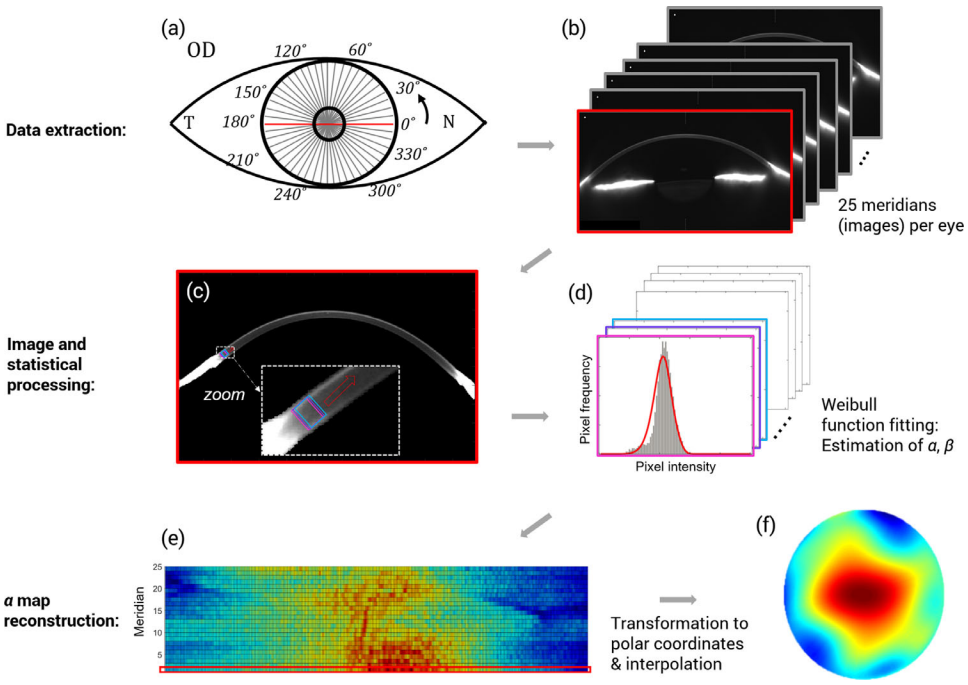

Figure 1. Main steps to obtain a corneal α parameter map from each Scheimpflug measurement. Diagram illustrates, using *gray lines*, the 25 meridians imaged by the Pentacam HR rotating camera (a) and the corresponding 25 images (b). The horizontal meridian is marked in *red* (a, b) as an example. After data extraction, each image is analyzed individually, first by segmenting the cornea and applying a moving ROI (c). For illustrative purposes, only the first three ROIs are shown with different colors along with a *red arrow* that indicates the continuity of the process across the segmented cornea (c). Second, the corresponding collection of histograms representing the pixel intensity distribution in each ROI are built (d). The probability density function (PDF) of the Weibull function is represented by the *red line* and fitted to the pixels in each ROI. The fit is performed by estimating the two parameters of the Weibull distribution (α and β), using the method of maximum likelihood (d). Finally, to construct a corneal α parameter map, the α values obtained from each frame in standard Cartesian coordinates (e) must be transformed to polar coordinates and interpolated to reach the final map (f). For illustrative purposes, the *red rectangle* in (e) indicates the α values corresponding to the first frame in (b) and the horizontal meridian in (a).

and posterior corneal boundaries, and the horizontal (lateral) dimension of the ROI had an optimized fixed size of 11 pixels.[18] The moving ROI covered approximately the central 8 mm of the cornea. To avoid undesired border effects (strong limbal/scleral reflections), the peripheral cornea was not included in the analysis.[18]

As in the previous work on keratoconus detection using Scheimpflug light intensity distribution,[17] pixels corresponding to a given ROI were modeled using the Weibull distribution function, defined as

$$f(x) = \frac{\beta}{\alpha}\left(\frac{x}{\alpha}\right)^{\beta-1} e^{-\left(\frac{x}{\alpha}\right)^{\beta}} \; if \; x \geq 0 \; or \; 0 \; otherwise$$

where the independent variable (x) represents pixel intensity, $\alpha > 0$ represents the scale parameter, and $\beta > 0$ represents the shape parameter. The parameters α and β are extracted from the Weibull probability density function of the tissue transparency. In general, a change in scale parameter α causes a shift in pixel intensity (x-axis), with higher α values corresponding to a brighter image (i.e., more scatter and less transparency), and vice versa. A change in shape parameter β affects the width of the pixel intensity distribution, with higher β values corresponding to large variations in pixel intensity within a given image or ROI, and low β values corresponding to very subtle intensity differences.[18] In this work, the focus is given to the α parameter, as it has repeatedly been proven to be more effective for keratoconus discrimination than β.[16,17]

To build corneal α and β parameter maps, data were transformed from Cartesian (x, y) to polar coordinates (r, θ) and interpolated, as well as smoothened using second-order Zernike polynomials, in agreement with previous research.[18] The complete methodology is illustrated in Figure 1.

Additionally, receiver operating characteristic (ROC) curves were used to determine the accuracy, precision, sensitivity (proportion of positives correctly identified), and specificity (proportion of negatives correctly identified as such) of the α parameter as a discriminator of subclinical keratoconus. Larger values of α are associated with keratoconus, as suggested by previous research.[17] About 12,500 data points conform

each corneal α parameter map. Considering the maximum value of such a large dataset as the discriminator parameter would be an oversimplification and not representative of the whole map. To overcome this limitation while still focusing on the higher values of α in each corneal map, the mean value of all α values in the fourth quartile (Q4; the highest 25% of all α values) was used in the ROC analysis. Other statistical estimates, such as the global mean, median, and maximum values, were initially considered but discarded due to their lower discriminative power between controls and subclinical keratoconus. For comparison purposes, the discriminative power of the Belin–Ambrósio enhanced ectasia display (BAD-D),[25] a clinical standard in the detection of subclinical keratoconus, was also evaluated.

The statistical analysis was performed using SPSS Statistics 25.0 for Windows (IBM Corp., Armonk, NY). The normality of each dataset was not rejected (Shapiro–Wilk test, $P > 0.05$). Furthermore, the one-way analysis of variance test (Bonferroni adjustment for multiple comparisons) was performed to determine differences in α and β parameters within groups. Mauchly's test of sphericity indicated that the assumption of sphericity had not been violated in any of the parameters under analysis.

Results

The corneal features and topometric indices of the different study groups (normal, subclinical keratoconus, and clinical keratoconus) provided in Table 1 are in agreement with previous clinical studies for subgroup classification.[26,27] Figure 2 shows an example of α and β parameters for a randomly selected participant from each group. As indicated by Table 2, α is a better parameter to discriminate within groups. The corresponding group mean α maps are shown in Figure 3.

As indicated by Figure 2 and shown in Figure 3, the mean light intensity distributions of each study group look very different, suggesting that it is possible to successfully differentiate between them. This is supported by the ROC analysis (Fig. 4), which confirmed a discrimination success of 97% (sensibility = 90.0% and specificity = 95%) when differentiating between subclinical keratoconus and control eyes for a cut-off value of 45.1 (Table 3).

The BAD-D index achieved lower discrimination success when screening subclinical keratoconus from control eyes (sensitivity = 85.0%, specificity = 85.0%, AUC = 0.80 with an optimized cut-off of 0.74; sensitivity = 50.0%, specificity = 95.0%, AUC = 0.60 with a standard cut-off of 1.60),[25] but performed equally well for screening clinical keratoconus from control eyes (sensitivity = 100%, specificity = 100%, AUC = 1.0). The logistic index for keratoconus (Logik), also based on corneal tomography but supported by artificial intelligence,[28] showed a better discriminating rate than BAD-D when screening subclinical keratoconus from control eyes (sensitivity = 85.0%, specificity = 95.0%, AUC = 0.90).

As indicated by Figures 2 and 3, differentiating between control and clinical keratoconus eyes using the DDA method is straightforward; however, the differences between controls and subclinical keratoconus are subtler. Figure 5 illustrates several cases of subclinical keratoconus to familiarize the reader with the appearance of these maps.

Table 1. Description of the Three Study Groups

	n (Mean ± SD)		
	Control ($n = 20$)	Subclinical Keratoconus ($n = 20$)	Keratoconus ($n = 20$)
Age	30 ± 5	28 ± 6	29 ± 7
Gender (female/male)	11/9	3/17	4/16
K_{max} (D)	44.0 ± 1.4	44.8 ± 1.6	56.0 ± 4.9
TCT (µm)	549 ± 26	534 ± 25	460 ± 28
I-S value (D)	0.19 ± 0.45	0.73 ± 0.56	7.68 ± 1.86
BAD-D	0.31 ± 0.47	1.60 ± 0.52	9.14 ± 2.30
Logik[27]	–0.99 ± 0.02	–0.47 ± 0.42	2.44 ± 0.51
ISV	14.65 ± 2.62	19.80 ± 6.25	93.15 ± 20.30
IHA	1.77 ± 1.42	7.11 ± 4.54	31.04 ± 24.19

K_{max}, maximal keratometry; TCT, thinnest corneal thickness; I-S value, inferior–superior value; Logik, logistic index for keratoconus detection and severity scoring; ISV, index of surface variance; IHA, index of height asymmetry.

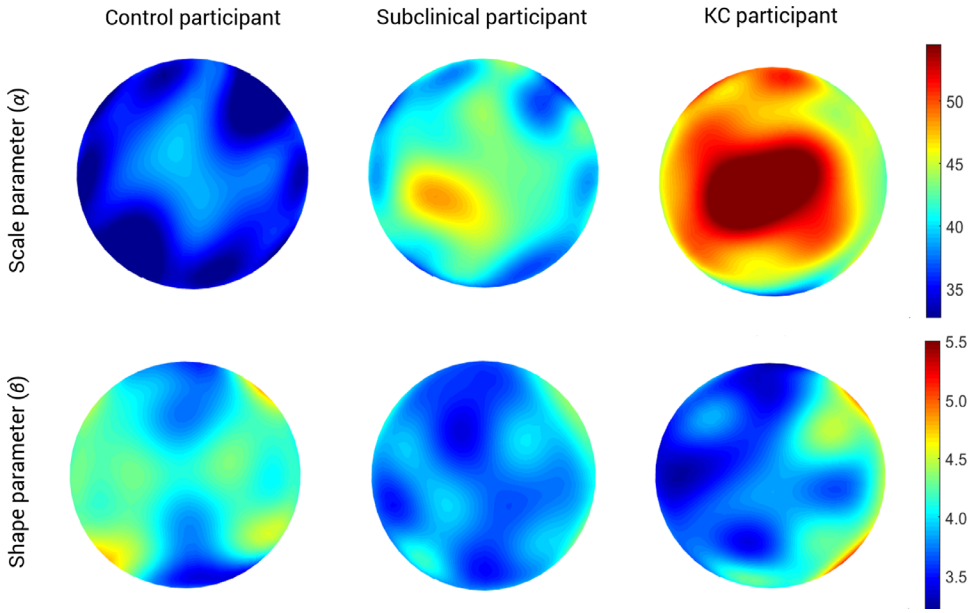

Figure 2. Example of α and β corneal maps for a randomly selected participant from each group. *Color bars* (α and β) are expressed in arbitrary units. KC, clinical keratoconus.

Table 2. Group Mean Values of α and β Parameters for the Three Study Groups

		Scale Parameter α			Shape Parameter β		
		Group Mean	Post Hoc Test		Group Mean	Post Hoc Test	
	Group	± SD (range), a.u.		*P*	± SD (range), a.u.		*P*
Mean map value	Control	39 ± 3 (34–47)	C vs. S	**0.037**	4.1 ± 0.5 (3.5–5.8)	C vs. S	1.00
	Subclinical	43 ± 4 (36–51)	S vs. KC	**0.020**	4.1 ± 0.6 (2.3–5.5)	S vs. KC	1.00
	Keratoconus	47 ± 5 (35–59)	KC vs. C	**<0.001**	3.9 ± 0.4 (3.1–4.7)	KC vs. C	0.53
Mean value in Q4	Control	41 ± 2 (38–47)	C vs. S	**<0.001**	4.3 ± 0.4 (3.8–5.8)	C vs. S	1.00
	Subclinical	50 ± 4 (44–53)	S vs. KC	1.00	4.1 ± 0.6 (2.4–5.5)	S vs. KC	**0.010**
	Keratoconus	50 ± 1 (44–59)	KC vs. C	**<0.001**	4.7 ± 0.7 (3.5–6.8)	KC vs. C	0.097

The group mean of the variable used for the ROC analysis (i.e., values in the fourth quartile [Q4] in each corneal map) is also included. Comparisons within groups were studied using one-way analysis of variance with Bonferroni adjustment for multiple comparisons. The corresponding post hoc test (multiple comparisons) is shown. Numbers in bold indicate a statistically significant difference. C, control; S, subclinical keratoconus; KC, clinical keratoconus.

Discussion

Diagnosing early-stage keratoconus is still a clinical challenge. This study shows that DDA reached 90.0% sensitivity, 95.0% specificity, and 0.97 AUC when distinguishing subclinical keratoconus from control eyes (Figs. 3, 4; Table 3), which is higher than the current tomography-based clinical standards.[29] Today, corneal tomography is the most commonly used method to screen for early keratoconus. Several diagnostic indices have been proposed to detect keratoconus based on Scheimpflug data, such as BAD-D, based on corneal thickness profile and elevation[25,30]; the Corneal Biomechanical Index (CBI) based on corneal thickness profile and corneal deformation parameters[31]; and the Tomographic and Biomechanical Index (TBI), a combination of Scheimpflug-based corneal tomography and biomechanics.[32] Although CBI and TBI outperform BAD-D in detecting early keratoconus,[32] BAD-D remains the clinical standard, probably due to its greater accessibility in clinical practice. In addition, BAD-D does not require mechanical stimulation of the cornea, unlike CBI and

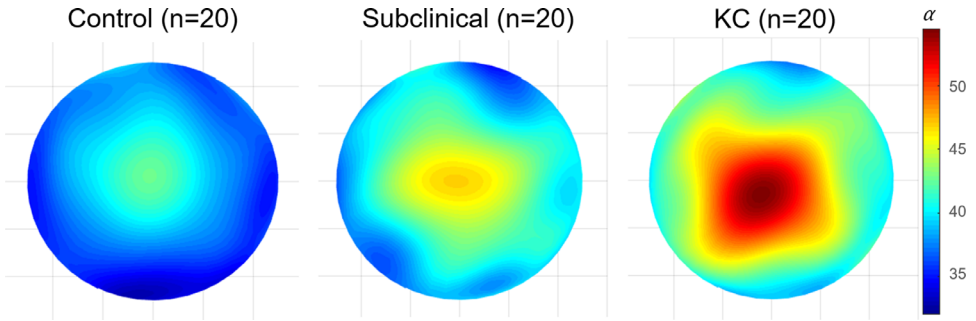

Figure 3. The mean distribution of α in the 8-mm central cornea of the three groups of participants. The *color bar* (α) is expressed in arbitrary units. KC, clinical keratoconus.

Table 3. Statistical Parameters That Determine the Efficacy of Diagnosing Subclinical and Clinical Keratoconus Using α Maps

	Sensitivity (%)	Specificity (%)	Accuracy (%)	Precision (%)	AUC	Cutoff Value (a.u.)
Control vs. subclinical keratoconus	90.0	95.0	92.5	94.7	0.97	45.1
Control vs. keratoconus	100	100	100	100	1.0	47.9

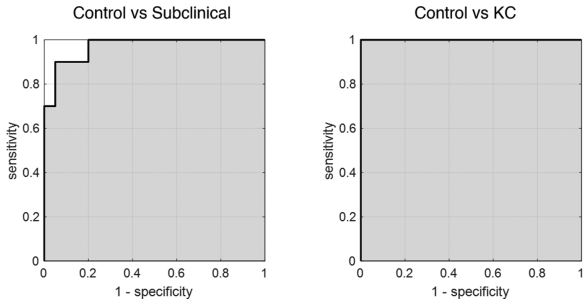

Figure 4. ROC curves indicating the discriminative power of the mean value in the fourth quartile (Q4) of the α parameter. Corresponding statistics are shown in Table 3.

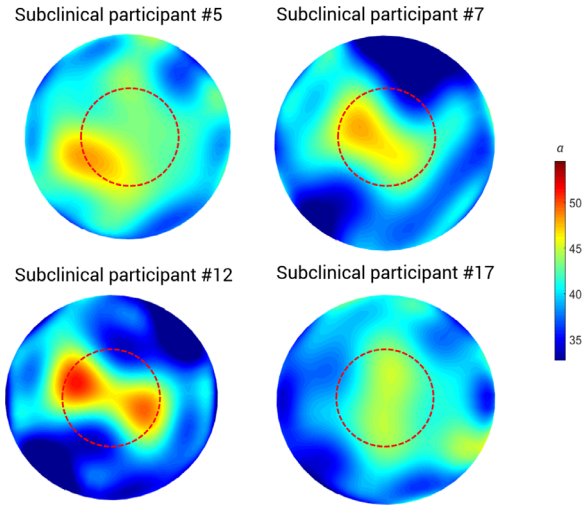

Figure 5. Examples of corneal α parameter maps for different participants from the subclinical keratoconus group. The *red dashed circle* demarcates the central 4-mm diameter. The *color bar* is expressed in arbitrary units.

TBI, making it more comfortable for the patients. Novel diagnostic indices to detect keratoconus from corneal tomographies based on artificial intelligence have been recently introduced, such as the Enhanced Tomographic Assessment to Detect Corneal Ectasia Based on Artificial Intelligence, the so-called Pentacam Random Forest Index (PRFI),[33] a computer-aided diagnosis system for early keratoconus detection,[27] and Logik.[28] Note that all of these Scheimpflug-based indices have something in common in that they exclusively evaluate the cornea at a macroscopic level, and all are based solely on macroparameters such as corneal curvature, corneal elevation, corneal thickness, or corneal deformation.

For the patients with subclinical keratoconus in the current report, all topographic and tomographic values were similar to those of the control group (Table 1). BAD-D reached 85.0% sensitivity, 85.0% specificity, and 0.80 AUC when discriminating between the control group and the subclinical keratoconus group, lower than that obtained with DDA (90.0% sensitivity, 95% specificity, and 0.97 AUC). This is in

accordance with the work of Koc et al.,[12] who suggested that densitometry analysis might be more effective to detect keratoconus in its early stages than traditional tomography.

Both traditional densitometry and DDA are based on the backscattering of light occurring by the cornea. The main advantage of DDA over traditional densitometry is its platform independence, as it can be applied to any Scheimpflug image, independent of the instrument used.[15] In addition, DDA is more versatile than traditional densitometry because it allows customization depending on the clinical purpose. In current work, for example, the method was optimized to discriminate between subclinical keratoconus and control eyes. Rather than considering the mean value of the entire corneal map, as is done in densitometry, the focus here was given to bright pixels because it is known that these are associated with keratoconus.[17] Consequently, the biomarker used in the ROC analysis was calculated using only the brightest pixels (i.e., those in the fourth quartile). When considering the mean α value over the entire corneal map, the difference between the control and subclinical keratoconus groups, although statistically significantly different ($P = 0.037$), was milder than when only considering the highest α values in the corneal map ($P < 0.001$). These are crucial methodological differences that must be considered in the proper clinical context when trying to distinguish individuals based on subtle differences.

DDA was already validated with rotating Scheimpflug cameras (Pentacam HR)[15,18] and Scheimpflug tonometry (Oculus Corvis ST),[16,18] showing a good level of agreement between devices.[15] DDA is based on the statistical Weibull modeling of the pixel intensity distribution of Scheimpflug images, which produces two parameters, α and β, of which the scale parameter (α) proved a useful biomarker to discriminate keratoconus.[16,17] In particular, in our previous report, the scale parameter from a single Scheimpflug image (i.e., without using corneal maps) achieved 76.0% sensitivity, 76.0% specificity, and 0.81 AUC when differentiating control from early to moderate keratoconus.[17] This result, validated with an out-of-sample dataset, improved to 100% sensitivity and 100% specificity when combined with central corneal thickness.[17] This earlier result highlights the importance of combining traditional tomographical parameters for keratoconus screening, such as corneal thickness or curvature, with tissue-related parameters, such as densitometry or the scale parameter (α). We believe that the current subclinical keratoconus detection system could still be improved to a system without misclassifications if, in addition to scale parameter α, other traditional morphological parameters, such as corneal thickness, were taken into consideration. This will require further validation, however.

The current work differs from the previous iterations of DDA to detect keratoconus in two key ways: (1) it considers the full corneal map, and (2) it uses the mean value of scale parameter α in the fourth quartile range as a discriminative parameter. Previous works have demonstrated that not only do higher values of scale parameter α (i.e., a less transparent stroma) correspond to keratoconus,[17] but also α displays regional changes over the cornea.[18] Because the current work aimed to discriminate subclinical keratoconus from controls, data analysis was focused on the fourth quartile range because this is the metric that was found to maximize the differences between these two groups (Table 2). As a part of a preliminary analysis, it was also considered to perform a regional analysis by concentric rings, after the standard Pentacam HR densitometry protocol. However, as Figure 5 illustrates, the highest values for scale parameter α do not consistently appear in the same corneal region. Considering only the central area of the cornea would, therefore, inevitably lead to information loss (as in, for example, subclinical participants 5 and 12 in Fig. 5). Similarly, considering only the outer ring of the cornea would, in most cases, remove the valuable higher values of α (Fig. 5). In both situations, the missing data would be crucial to accurately distinguish the very subtle difference between subclinical keratoconus and control eyes, so restricting the analysis area would not help discriminate between these two groups.

The independence of corneal thickness from α and β parameters was demonstrated in previous work in keratoconic and healthy eyes using Scheimpflug imaging.[17] Here, a bootstrap analysis was performed, which indicated that not only are macroscopic and microscopic parameters independent from each other but corneal thickness is also not a confounding factor that affects the calculation of α and β.[17]

A limitation of the current study is that the process of data extraction might be time consuming. Pentacam HR software, in contrast to that of other Scheimpflug devices such as the Corvis ST, cannot automatically export the images corresponding to each corneal meridian. Consequently, the process of image capture must be done manually. In addition, future external validation studies with out-of-sample datasets are necessary. In this context, it would be interesting to compare the reported diagnostic power with that from the PRFI.[6,22,33]

In conclusion, we investigated the usefulness of corneal light backscatter analysis to discriminate subclinical keratoconus from control eyes, upgrading the results previously reported in the literature.

Acknowledgments

Supported by funding from the National Science Centre (Poland) under the OPUS 19 funding scheme (project no. 2020/37/B/ST7/00559).

Disclosure: **A. Consejo,** None; **M. Jiménez-García,** None; **I. Issarti,** None; **J.J. Rozema,** None

References

1. Hashemi H, Heydarian S, Hooshmand E, et al. The prevalence and risk factors for keratoconus: a systematic review and meta-analysis. *Cornea*. 2020;39(2):263–270.
2. Godefrooij DA, De Wit GA, Uiterwaa CS, et al. Age-specific incidence and prevalence of keratoconus. *Am J Ophthalmol*. 2017;175:169–172.
3. Gain P, Jullienne R, He Z, et al. Global survey of corneal transplantation and eye banking. *JAMA Ophthalmol*. 2016;134(2):167–173.
4. Ambrósio R, Randleman JB. Screening for ectasia risk: what are we screening for and how should we screen for it? *J Refract Surg*. 2013;29(4):230–232.
5. Pérez JF, Marcos AV, Peña FJ. Early diagnosis of keratoconus: what difference is it making? *Br J Ophthalmol*. 2014;98(11):1465–1466.
6. Ambrósio R. Post-LASIK ectasia: twenty years of a conundrum. *Semin Ophthalmol.* 2019;34(2):66–68
7. Seiler T, Quurke AW. Iatrogenic keratectasia after LASIK in a case of forme fruste keratoconus. *J Cataract Refract Surg*. 1998;24(7):1007–1009.
8. Randelman JB, Russel B, Ward MA, et al. Risk factors and prognosis for corneal ectasia after LASIK. *Ophthalmology*. 2003;110:267–275.
9. Mas Tur V, MacGregor C, Jayaswal R, O'Brart D, Maycock N. A review of keratoconus: diagnosis, pathophysiology, and genetics. *Surv Ophthalmol*. 2017;62(6):770–783.
10. Jiménez-García M, Dhubhghaill SN, Koppen C, et al. Baseline findings in the Retrospective Digital Computer Analysis of Keratoconus Evolution (REDCAKE) project. *Cornea*. 2021;40(2):156–167.
11. Ruiseñor Vázequez PR, Galetti JD, Minguez N, et al. Pentacam Scheimpflug tomography findings in topographically normal patients and subclinical keratoconus cases. *Am J Ophthalmol*. 2014;158:32–40.
12. Koc M, Tekin K, Tekin MI, et al. An early finding of keratoconus: increase in corneal densitometry. *Cornea*. 2018;37(5):580–586.
13. Lopes B, Ramos IC, Ambrósio R. Corneal densitometry in keratoconus. *Cornea*. 2014;33:1282–1286.
14. Jiménez-García M, Dhubhghaill SN, Consejo A, et al. Scheimpflug densitometry in keratoconus: a new method of visualizing the cone. *Cornea*. 2021;40(2):194–202.
15. Consejo A, Jiménez-García M, Rozema JJ. Age-related corneal transparency changes evaluated with an alternative method to corneal densitometry. *Cornea*. 2021;40(2):215–222.
16. Consejo A, Gławdecka K, Karnowski K, et al. Corneal properties of keratoconus based on Scheimpflug light intensity distribution. *Invest Ophthalmol Vis Sci*. 2019;60(8):3197–3203.
17. Consejo A, Solarski J, Karnowski K, et al. Keratoconus detection based on a single Scheimpflug image. *Transl Vis Sci Technol*. 2020;9(7):36.
18. Consejo A, Alonso-Caneiro D, Wojtkowski M, Vincent SJ. Corneal tissue properties following scleral lens wear using Scheimpflug imaging. *Ophthalmic Physiol Opt*. 2020;40(5):595–606.
19. Rozema JJ, Atchison DA, Tassignon MJ. Statistical eye model for normal eyes. *Invest Ophthalmol Vis Sci*. 2011;52(7):4525–4533.
20. Rozema JJ, Koppen C, Bral N, et al. Changes in forward and backward light scatter in keratoconus resulting from corneal crosslinking. *Asia Pac J Ophthalmol (Phila)*. 2013;2(1):15–19.
21. John AK, Asimellis G. Revisiting keratoconus diagnosis and progression classification based on evaluation of corneal asymmetry indices, derived from Scheimpflug imaging in keratoconic and suspect cases. *Clin Ophthalmol*. 2013;7:1539–1548.
22. Salomão MQ, Hofling-Lima AL, Esporcatte LP, et al. Ectatic diseases. *Exp Eye Res*. 2021;202:108347.
23. Rabinowitz YS, Rasheed K. KISA% index: a quantitative videokeratography algorithm embodying minimal topographic criteria for diagnosing keratoconus. *J Cataract Refract Surg* 1999;25:1327–1335.
24. Belin MW, Duncan JK. Keratoconus: the ABCD Grading System. *Klin Monbl Augenheilkd*. 2016;233:701–707.
25. Villavicencio OF, Gilani F, Henriquez MA, et al. Independent population validation of the Belin/Ambrosio enhanced ectasia display: implications for keratoconus studies and screening. *Int J Keratoconus Ectatic Corneal Dis*. 2014;3(1):1.
26. Hidalgo IR, Rozema JJ, Saad A, et al. Validation of an objective keratoconus detection system

implemented in a Scheimpflug tomographer and comparison with other methods. *Cornea*. 2017;36(6):689–695.
27. Issarti I, Consejo A, Jiménez-García M, et al. Computer aided diagnosis for suspect keratoconus detection. *Comput Biol Med*. 2019;109:33–42.
28. Issarti I, Consejo A, Jiménez-García M, et al. Logistic index for keratoconus detection and severity scoring (Logik). *Comput Biol Med*. 2020;122:103809.
29. Ruiseñor Vázquez PR, Galletti JD, Minguez N, et al. Pentacam Scheimpflug tomography findings in topographically-normal patients and subclinical keratoconus cases. *Am J Ophthalmol*. 2014;158:32–40.
30. Ambrósio R, Caiado AL, Guerra FP, et al. Novel pachymetric parameters based on corneal tomography for diagnosing keratoconus. *J Refract Surg*. 2011;27(10):753–758.
31. Vinciguerra R, Ambrósio R, Elsheikh A, et al. Detection of keratoconus with a new biomechanical index. *J Refract Surg*. 2016;32:803–810.
32. Ambrósio R, Lopes BT, Faria-Correia F, et al. Integration of Scheimpflug-based corneal tomography and biomechanical assessments for enhancing ectasia detection. *J Refract Surg*. 2017;33(7):434–443.
33. Lopes BT, Ramos IC, Salomão MQ, et al. Enhanced tomographic assessment to detect corneal ectasia based on artificial intelligence. *Am J Ophthalmol*. 2018;195:223–232.